FEBS Letters 583 (2009) 2054–2060

journal homepage: www.FEBSLetters.org

Reversible unfolding of dimeric phosphofructokinase-2 from *Escherichia coli* reveals a dominant role of inter-subunit contacts for stability

Mauricio Baez, Jorge Babul *

Departamento de Biología, Facultad de Ciencias, Universidad de Chile, Santiago, Chile

ARTICLE INFO

Article history:
Received 6 March 2009
Revised 2 May 2009
Accepted 15 May 2009
Available online 22 May 2009

Edited by Judit Ovádi

Keywords:
Reversible unfolding
Subunit interaction
Folding intermediate
Dimer–monomer transition
Ribokinase superfamily
Bimolecular domain

ABSTRACT

Escherichia coli **phosphofructokinase-2 (Pfk-2) is a homodimer whose subunits consist of a large domain and an additional β-sheet that provides the interfacial contacts between the subunits, creating a β-barrel flattened-like structure with the adjacent subunit's β-sheet. To determine how the structural organization of Pfk-2 determines its stability, the reversible unfolding of the enzyme was characterized under equilibrium conditions by enzymatic activity, circular dichroism, fluorescence and hydrodynamic measurements. Pfk-2 undergoes a cooperative unfolding/dissociation process with the accumulation of an expanded and unstructured monomeric intermediate with a marginal stability and a large solvent accessibility with respect to the native dimer.**

1. Introduction

Phosphofructokinase-2 (Pfk-2) from *Escherichia coli* is a member of the ribokinase superfamily, a group of sugar and vitamins kinases formed by a common α/β/α domain [1]. In sugar and sugar phosphates kinases, such as ribokinase [2], tagatose-6-P kinase [3], 2-keto-3-deoxygluconate kinase [4] and Pfk-2 [5], there is an additional structure that forms a lid for the active site. This structure is a four stranded β-sheet inserted non-sequentially near the N-terminal end of the conserved α/β/α domain. On the other hand, vitamins and small molecules kinases are mainly formed by the conserved α/β/α domain since their structures lack the additional β-sheet structure [6]. Pyridoxal kinases correspond to such kind of kinases and have been characterized as active monomers [7], although a dimer can be observed in the protein crystal [8,9]. The guanidine hydrochloride (GdnHCl) induced unfolding of pyridoxal kinase from human and sheep brain, was reported as a two-state reversible equilibrium with calculated stability values of 1.2 kcal mol^{-1} [10] and 1.55 kcal mol^{-1} [11] respectively. These values indicate that in both cases the conserved α/β/α domain behaves as single cooperative unit exhibiting a marginal stability. However, in the case of sugar and sugar phosphate kinases, such as *E. coli* Pfk-2, is not known how the β-sheet insertion cooperates to bring about the stability of the native structure.

Light scattering and gel filtration analyses [12,13] have shown that *E. coli* Pfk-2 is primarily a dimer in solution, which quaternary structure is required for enzymatic activity [12,14]. As shown by its crystal structure (PDB ID code 3CQD), each subunit can be divided in two parts: the conserved α/β/α domain and the additional β-sheet structural element that protrudes from it. In Pfk-2 and in close family homologues, the additional β-sheet structure works as lid for the active site and also creates the interaction surface between the subunits, forming an intertwined interface denominated β-clasp [8]. Thus, Pfk-2 seems to be stabilized by two domains: the β-clasp interface and the conserved α/β/α domain that accounts for the mayor part of the intermolecular contacts of each subunit. In this kind of dimers both domains are separated by the active site, which is mainly self-contained in each subunit [8].

The GdnHCl unfolding of Pfk-2 was recently studied in order to obtain information regarding the structure of the separated subunits [14]. The dissociation of the enzyme originates a semi structured monomer with an expanded volume. However, a thermodynamic analysis of the unfolded transitions has not been explored in detail. In this work, we describe the reversible effect of GdnHCl on the dissociation and unfolding of Pfk-2 following

Abbreviations: Pfk-2, phosphofructokinase-2; GdnHCl, guanidine hydrochloride; ANS, 8-anilino-1-naphthalene sulfonic acid; DTT, dithiotreitol; SEC, size exclusion chromatography; CD, circular dichroism spectroscopy; DLS, dynamic light scattering; Cm, guanidine hydrochloride concentration at the middle of the observed property change; Rs, Stokes radius

* Corresponding author. Fax: +56 2 272 6006.
E-mail addresses: jbabul@uchile.cl, jbabul@gmail.com (J. Babul).

0014-5793/$36.00
doi:10.1016/j.febslet.2009.05.034

enzymatic activity, intrinsic tryptophan fluorescence and circular dichroism. Moreover, the hydrodynamic properties Pfk-2 were followed by size exclusion chromatography and dynamic light scattering measurements. The simplest model to describe the global unfolding of Pfk-2 is a three-state unfolding reaction $N_2 \leftrightarrow 2I \leftrightarrow 2U$, characterized by a semi-unstructured monomeric intermediate with an expanded volume. The energetic parameters extracted from the three-state unfolding model, indicate that the inter-subunit contact between the four-stranded β-sheets extra domain confers the global stability to Pfk-2 since the isolated subunits present a reduced stability with respect to the native dimer. Taken together the physical characteristics of the monomeric intermediate and its stability, is postulated that the conserved α/β/α domain and the β-sheet insertion are thermodynamically coupled in the dimeric structure of Pfk-2.

2. Materials and methods

2.1. Pfk-2 purification and storage

E. coli Pfk-2 was purified and stored as described by Cabrera et al. [15]. Previous to the unfolding or refolding experiments, the storage buffer was changed to the standard buffer (50 mM Tris pH 7.8, 5 mM $MgCl_2$ and 10 mM dithiotreitol (DTT)) by using a HiTrap desalting column (Amersham Biosciences, Uppsala, Sweden), before a 3 h dialysis in the same buffer. The enzyme was concentrated by using a centricon-60 concentrator (Amicon, Berverly, USA). Protein concentration was determined by the Bradford assay (Bio-Rad) and is expressed in terms of the monomer concentration.

2.2. Pfk-2 unfolding and refolding

For the refolding experiments, the enzyme was first exposed to 3 M GdnHCl (Pierce, molecular biology grade) for at least 5 h at 20 °C. Under this condition Pfk-2 was completely unfolded, as indicated by its catalytic activity, circular dichroism spectroscopy (CD) and intrinsic fluorescence measurements. The refolding curve was obtained diluting the unfolded enzyme to several GdnHCl concentrations in the standard buffer. Under these conditions equilibrium was achieved after 5 h of incubation at 20 °C. The unfolding curves were constructed by diluting native Pfk-2 to several GdnHCl concentrations. In this case equilibrium was obtained after 48 h at 20 °C. GdnHCl concentrations were prepared as described by Pace [16].

2.3. Enzyme assays

Phosphofructokinase enzymatic activity was measured spectrophotometrically by a coupled assay as described by Babul [17]. The activity assay began by dilution of a 1 μl aliquot containing the enzyme and GdnHCl into 700 μl of assay mixture. Since this procedure implies the dilution of GdnHCl, renaturation should be expected. To determine the renaturation yield of Pfk-2 during the enzymatic assay, the enzyme was unfolded with GdnHCl and refolded into the assay mixture to bring about a protein concentrations of 0.004 μM (the protein concentration used in the coupled assay). Under these conditions, substrates were added at several times after refolding was initiated and the enzymatic activity was followed. The activity was only about 3% with respect to that measured with samples that were not previously denatured.

2.4. Intrinsic and ANS fluorescence

Measurements were done in a Perkin–Elmer LS 50 spectrofluorimeter. Protein samples at several GdnHCl concentrations were excited at 295 nm to limit the fluorescence to the single tryptophan per monomer of Pfk-2 (Trp-88). The emission spectra were recorded from 300 to 480 nm using emission and excitation slits of 5 nm. Stock 8-anilino-1-naphthalene sulfonic acid (ANS) solutions (Molecular Probes, Eugene, USA) were prepared in methanol and its concentration was determined using a ε of 7800 M^{-1} cm^{-1} at 372 nm. The Pfk-2 samples refolded and unfolded at different GdnHCl concentrations contained 80 μM ANS. The mixture was incubated for 48 h in the dark. Samples prepared in this way were excited at 380 nm and the emission recorded from 400 to 580 nm.

2.5. Circular dichroism spectroscopy

Far UV CD spectra were acquired in a Jasco J600 dichrograph, employing 1 mm cell. Each spectrum resulted from the accumulation of three scans (bandwidth 1 mm, scan rate 20 nm min^{-1}) between 210 and 260 nm (the high absorbance of 5–10 mM DTT did not allow to record spectra below 210 nm).

2.6. Size exclusion chromatography

Size exclusion chromatography (SEC) equilibrium experiments were performed using a Water Breeze HPLC system equipped with a Bio-Rad exclusion column (Bio-Sil SEC 250 gel filtration, 300 × 7.8 mm). The column was equilibrated with 60 ml of the mobile phase containing 0.2 M KCl in standard buffer with the same GdnHCl concentration of that of the sample to be injected. Calibration was performed by using the proteins provided by the manufacturer of the column (Vitamin B-12, 1.35 kDa, 8.5 Å Stokes radius (Rs); horse myoglobin, 17 kDa, 19 Å Rs; chicken ovalbumin, 44 kDa, 30.5 Å Rs; bovine gamma globulin, 158 kDa, 41.8 Å Rs; and bovine thyroglobulin 670 kDa, 85 Å Rs). Protein elution volumes were converted to Rs values using the linear relationship obtained with the molecular-mass markers). The column temperature was adjusted with a water jacket at 20 °C. Protein elution was followed at 220 and 280 nm. The concentration of the injected protein ranged between 2 and 20 μM.

2.7. Dynamic light scattering experiments

The Stokes radius (Rs) of Pfk-2 in 50 mM Tris buffer pH 8, 5 mM $MgCl_2$, 10 mM DTT incubated at different GdnHCl concentrations for 24 h at 20 °C, was determined by dynamic light scattering (DLS) using a DynaPro MSTC014 (Protein Solutions, Lakewood, NJ, USA) at a protein concentration of 14 μM. All solutions were centrifuged at 13 600×*g* for 30 min prior to data collection. The protein concentration of the samples was measured before and after these treatments and no significant loss of sample was observed. Data were acquired by accumulation of 18 readings of 5 s with detector sensitivity set to 80%. The particle size distribution was calculated by using the 'regularization' method provided with the DYNAMICS software, supplied with the instrument. The residual scattering intensity (intensity scattered by the protein without solvent contribution) was also determined.

2.8. Data analysis

CD unfolding curves were analyzed according to a three-sate model:

$$N_2 \overset{K_1}{\Longleftrightarrow} 2I \overset{K_2}{\Longleftrightarrow} 2U$$

where N_2 represents the native state dimer, I is a monomeric intermediate and U, is the unfolded polypeptide.

The changes in the Gibbs energy expressed in the unfolding sense of the reaction for the intermediate unfolding (ΔG_2) and the native dimer unfolding (ΔG_1) are defined as $\Delta G_2 = -RT \ln K_2$

and $\Delta G_1 = -RT \ln K_1$ respectively, were R is the gas constant in kcal mol^{-1} K^{-1} and T is the temperature in Kelvin degrees. The change in free energy is assumed to be a linear function of denaturant molar concentration (D):

$$\Delta G_1 = \Delta G_1^o + m_1 D$$
$$\Delta G_2 = \Delta G_2^o + m_2 D$$

where $\Delta G^o_{(x)}$ is the free energy change extrapolated to zero denaturant concentration and m_1 and m_2 are the free energy dependence of the denaturant concentration for the native dimer (ΔG_1^o, m_1) and the intermediate (ΔG_2^o, m_2) respectively. The fraction of unfolded state (f_u), intermediate state (f_i) and native state (f_n) are related to the equilibrium constant K_1 and K_2 by:

$$f_u = \frac{K_1 K_2 \left(-(1+K_2) + \sqrt{(1+K_2)^2 + 8Pt/K_1} \right)}{4Pt} \quad (1)$$

$$f_i = f_u / K_2 \quad (2)$$

$$f_n = 1 - f_i - f_u \quad (3)$$

where Pt is the total protein concentration in terms of monomers.

The observed signal (y_{obs}) was assumed to be dependent on the population of species according to $y_{obs} = y_u f_u + y_i f_i + y_n f_n$, where y_u, y_i and y_n are the specific signals of the unfolded, intermediate and native protein, respectively. The dependence of the baseline signal for the unfolded and native species with the denaturant concentration was incorporated in the calculation procedure. The energetic parameters obtained from enzymatic activity and intrinsic fluorescence measurements were calculated by fitting the data to a single transition according to a $N_2 \leftrightarrow 2I$ model as established by Apiyo et al. [18].

3. Results

3.1. Folding pathway of Pfk-2 under equilibrium conditions

The GdnHCl-induced unfolding of Pfk-2 was followed by CD, intrinsic fluorescence and enzymatic activity measurements (Fig. 1). Since the activity recovery after refolding was found to be at least 90% in the full range of GdnHCl concentrations (inset, Fig. 1C), we assume that the irreversible formation of aggregates is not a preferred reaction pathway under our experimental conditions. Two clear transitions separated by a wide plateau are seen when the secondary structure changes due to unfolding are monitored by CD (Fig. 1A), suggesting the presence of an intermediate state near to 0.5 M GdnHCl. The first transition occurs from 0.15 to 0.4 M GdnHCl with a middle point about 0.23 M at a protein concentration of 5 μM. This transition accounts for the 70% of the overall difference between the CD signal of native and unfolded protein observed at 220 nm. The second transition occurs between 0.8 and 2.8 M GdnHCl, and ends with the total unfolding of the enzyme as judged by the CD spectrum of Pfk-2 at 3 M GdnHCl (inset, Fig. 1A).

Conversely, the unfolding curves followed by the two other independent structural probes, intrinsic fluorescence (Fig. 1B) and enzymatic activity (Fig. 1C), show only one transition which is superposable with the first CD transition, but failed to reproduce the second transition observed from 0.8 to 2.8 M GdnHCl. Consequently, the intermediate accumulated around 0.5 M GdnHCl is characterized by a residual secondary structure, lack of enzymatic activity and a non-native environment of Trp-88. The refolding curves obtained by dilution of the unfolded Pfk-2 from 3 M GdnHCl show a good superposition with the unfolding curves described above (Fig. 1A–C). Accordingly, the fluorescence and CD spectra obtained for the native protein were almost completely recovered after refolding of Pfk-2 to 0.1 M GdnHCl (insets, Fig. 1) indicating that the unfolding of dimeric Pfk-2 is a fully reversible process.

To test if the first transition observed with the loss of secondary structure represents a concerted unfolding and dissociation steps, the equilibrium unfolding transitions were assayed using several protein concentrations. As shown in the inset of Fig. 2, the unfolding transitions followed by enzymatic activity and intrinsic fluorescence shifted their guanidine hydrochloride concentration at the middle of the observed property change (Cm) values to higher concentrations of GdnHCl upon increasing the protein concentration. The first transition detected by CD was also shifted to elevated concentrations of GdnHCl with increasing protein concentrations. The second CD transition (Cm ~ 1.5 M GdnHCl) seems not to be affected by the protein concentration (Fig 2).

Therefore, we can conclude that the simplest model to describe the global unfolding of Pfk-2 is a three-state unfolding reaction with a monomeric intermediate: $N_2 \leftrightarrow 2I \leftrightarrow 2U$. Table 1 shows the energetic parameters obtained by fitting the CD data to this model by the procedure described under Section 2. The change of free energy associated with the $N_2 \leftrightarrow 2I$ step, ΔG_2^o, was 12.2 ± 0.9 kcal mol^{-1} and that corresponding to $I \leftrightarrow U$ step, ΔG_2^o,

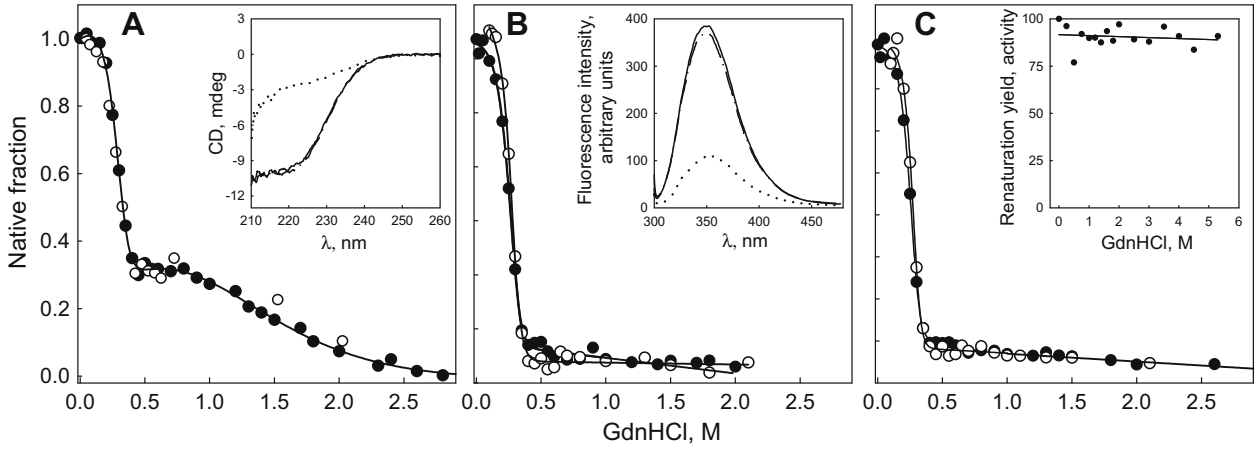

Fig. 1. Unfolding and refolding of Pfk-2. (A) Relative changes of ellipticity at 222 nm. (B) Tryptophan intrinsic fluorescence at 350 nm. (C) Enzymatic activity as a function of the GdnHCl concentration. The empty and filled symbols correspond to the refolding and unfolding reactions respectively. The solid lines represent the curve fit to the $N_2 \leftrightarrow 2I \leftrightarrow 2U$ (A), and $N_2 \leftrightarrow 2I$ (B, C) unfolding models from which the thermodynamic parameters were derived. Inset: (A) and (B) far-UV circular dichroism and tryptophan emission spectra, respectively, of the (—) native, (–·–·–) refolded and (. . .) unfolded Pfk-2. Inset (C), recovery of the enzymatic activity from several GdnHCl concentrations (indicated in the figure) upon dilution to 0.1 M. Spectra and activity measurements were obtained with 3.3 μM protein at 20 °C.

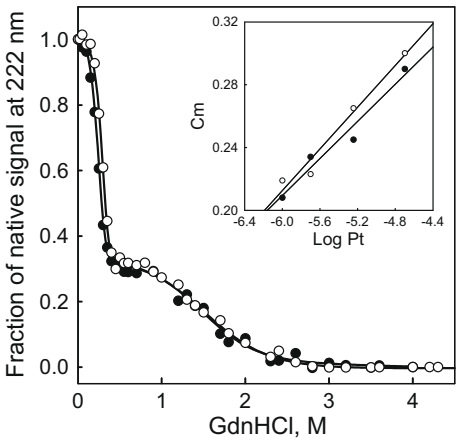

Fig. 2. Effect of protein concentration on Pfk-2 folding. Relative changes in the ellipticity at 222 nm were plotted as function of GdnHCl concentration at two protein concentrations, 4.7 μM (●) and 19 μM (○). The solid lines represent the fitting of the experimental values to an unfolding mechanism with a monomeric intermediate. Inset: effect of protein concentration on the Cm of the unfolding curves followed by (■) enzymatic activity and (□) intrinsic fluorescence. The solid lines indicate the best fit to a linear semi logarithmic equation for a model with an unfolding-dissociation coupled process ($N_2 \leftrightarrow 2I$). The linear regression (r^2) values obtained from the enzymatic activity and intrinsic fluorescence as function of the logarithm of the protein concentration were 0.968 and 0.958 respectively.

was ~2.4 kcal mol^{-1}. Similar values were obtained for the $N_2 \leftrightarrow 2I$ step from fluorescence and enzymatic activity measurement (11.9 ± 0.2 and 12.1 ± 0.6 kcal mol^{-1}, respectively). These results indicate that the global change of the free energy between the native dimer and the unfolded monomer is about 17 kcal mol^{-1} ($\Delta G_2^o + 2\Delta G_2^o$), with the unfolding and dissociation step ($N_2 \leftrightarrow I$) contributing with 70% of the overall free energy change. The *m*-values obtained for the $N_2 \leftrightarrow 2I$ and $I \leftrightarrow U$ steps were ~17 ± 2 and 1.7 kcal mol^{-1} M^{-1}, respectively. Since the empiric *m*-value is related to the difference in accessible surface area between two states [19], our results indicate that 90% of the total change in accessible surface area between the native and unfolded state occurs in the first step of unfolding, $N_2 \leftrightarrow 2I$.

As demonstrated from the early studies of Daniel and Weber [20] the quantum yield of ANS suffers an increment and its emission maximum shifts to the blue when it binds to solvent exposed hydrophobic regions in proteins. Fig. 3A shows the variation of the ANS emission maximum of and its emission area as function of the GdnHCl concentration. The ANS emission area shows an asymmetrical bell-shape dependence with the chaotropic agent concentration, which was superimposable for the refolding and unfolding curves. This behavior resembles the fractional population of the monomeric intermediate (Fig. 3B) calculated from Eqs. (1–3), indicating that the intermediate detected by CD presents a solvent exposed hydrophobic patch observed as an increment of the ANS emission area. However, it is clear from Fig. 3A that the variation of the emission maximum does not follow the variation of the ANS emission area. As is observed from 0.5 to 1.8 M GdnHCl, the emission maximum value of ANS stays constant at 460 nm and increases to 510 nm at 3 M, with small changes in its emission area. This behavior suggests the presence of additional intermediate species, different from the one inferred from the CD and the ANS fluorescence area measurements, which could accumulate at higher GdnHCl concentrations.

Table 1
Thermodynamic parameters calculated from the unfolding of Pfk-2 at pH 7.8 and 20 °C.

	Enzimatic activity[a]	Tryptophan fluorescence[a]	Circular dichroism[b]	
	$N_2 \leftrightarrow 2I$	$N_2 \leftrightarrow 2I$	$N_2 \leftrightarrow 2I$	$I \leftrightarrow U$
ΔG^o (kcal mol^{-1})	12.1 ± 0.6	11.9 ± 0.2	12.2 ± 0.9	2.4
$-m$ (kcal mol^{-1} M^{-1})	19.6 ± 2.2	19.5 ± 0.5	17 ± 2.8	1.66

[a] Analyzed in terms of a two state (dimer to monomer) transition. Error values correspond to three or more independent measurements.
[b] Analyzed in terms of a three state transition with a monomeric intermediate. Error values correspond to three or more independent measurements.

3.2. Hydrodynamic characterization of the intermediate obtained in presence of GdnHCl

SEC and DLS measurements were used to determine the Rs of the native, intermediate and unfolded species in the unfolding pathway of Pfk-2. Fig. 4A shows the elution profile of Pfk-2 obtained at different GdnHCl concentrations after injecting a 50 μl sample of the protein onto a column equilibrated at the same GdnHCl concentration. The calculated Rs of Pfk-2 at 0 M GdnHCl was 34.9 Å according to SEC (Fig. 4A) and 36.5 Å according to DLS measurements (Fig. 5). The elution volume of Pfk-2 increases, as a single peak, in the short interval before the first transition (see

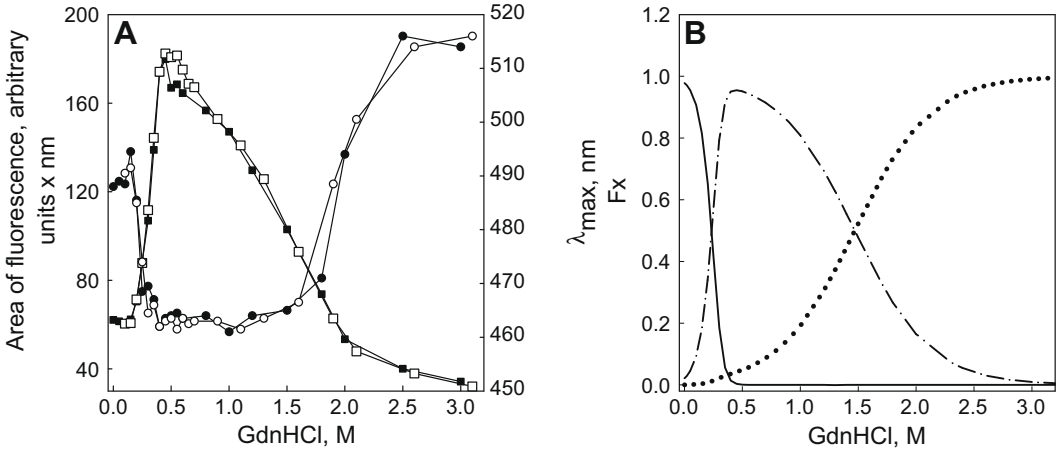

Fig. 3. Population fraction of Pfk-2 species and change in the ANS fluorescence area and maximum of emission as a function of the GdnHCl concentration. (A) The ANS fluorescence area (■, □) and the emission maximum (●, ○) are plotted as function of the GdnHCl concentration for the unfolding (black symbols) and the refolding (white symbols) equilibrium curves. (B) Fractions of native dimer (—), monomeric intermediate (–·–·–) and unfolded state (. . .), calculated from the energetic parameters of Table 1. The simulation was performed using the same protein concentration as in the ANS experiment (2 μM).

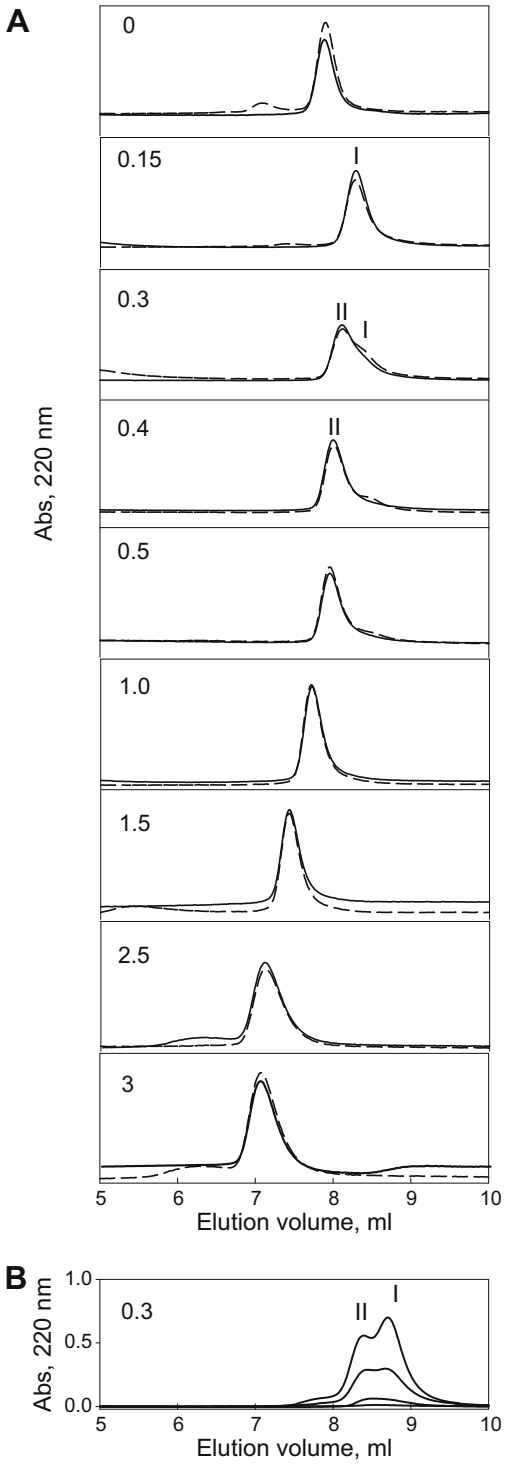

Fig. 4. Elution profiles of Pfk-2 at different GdnHCl and protein concentrations obtained by size exclusion chromatography. (A) Protein samples (2 μM) were injected into the column equilibrated at the indicated GdnHCl concentrations. The continuous lines correspond to the elution profile of the native protein incubated with several GdnHCl concentration and the dashed lines represent the elution profile obtained with samples previously unfolded with 3 M of GdnHCl and incubated with the GdnHCl concentrations indicated in the figure. (B) Elution profile of Pfk-2 obtained with 1, 2, 18 and 33 μM of protein injected into a column equilibrated at 0.3 M GdnHCl. At 0.3 M GdnHCl, peak I and II species are indicated.

Fig. 4A). For simplicity, we will refer to this species as peak I. However, as indicated by the shaded area that covers the pre-transition zone (Fig. 5), the elution volume increment was not correlated with a decrease of the Rs measured by DLS, suggesting that peak

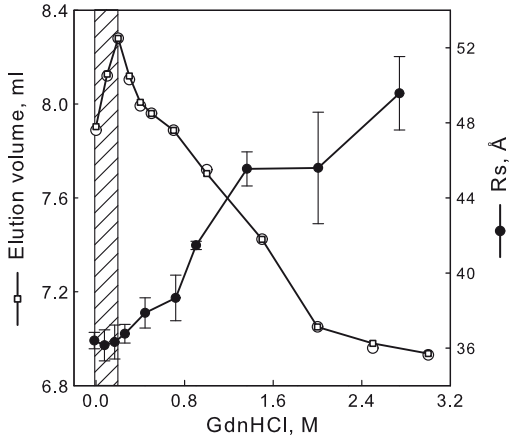

Fig. 5. Effect of GdnHCl on the hydrodynamic properties of Pfk-2. Pfk-2 elution volumes obtained by SEC under (□) unfolding and (○) refolding conditions. The shaded zone represents the pre-transition region observed with the unfolding and refolding curves of Pfk-2 where an increased elution volume was detected without the appearance of a second peak. In this region, the Rs radius obtained by DLS (●) does not show a significant variation. The protein concentration was 15 μM in both experiments.

I is not a product of the dissociation of dimeric Pfk-2. This is consistent with the effect of protein concentration on the equilibrium unfolding curves obtained by enzymatic activity and spectroscopic measurements, which indicates that the transition between dimer and monomers does not occur at GdnHCl concentrations lower than 0.15 M. Therefore, the elution volume increment obtained by SEC at the pre-transition region could be due to anomalous protein–matrix interactions and not to a dissociation event.

Coincident with the first transition region (CD signal between 0.15 and 0.5 M GdnHCl) emerges a new peak (peak II) with a Rs higher than peak I, as indicated by its lower elution volume (Fig. 4A). The population of peak II increases from 0.15 to 0.5 M GdnHCl and seems to predominate at 0.5 M, condition under which the maximum accumulation of the equilibrium intermediate is obtained (Fig. 3). Since unfolding and dissociation of Pfk-2 ($N_2 \leftrightarrow 2I$) occurs within this range of GdnHCl concentrations, we tested if the relative equilibrium population of both species could be modified by injecting samples of different protein concentrations into the column (Fig. 4B). With column and samples equilibrated at 0.3 M GdnHCl, the population of peak I increases over peak II upon increasing the protein concentration from 1 to 18 μM Pfk-2. On the other hand, at 0.15 M GdnHCl a proportional increment the area of peak I is observed without changes in the elution volume, supporting the fact that peak I corresponds to a dimer and peak II corresponds to the monomeric intermediate (data not shown). Some chromatograms show minor additional peaks at low elution volumes which could correspond to Pfk-2 aggregates (Fig. 4, panels at 0, 2.5, and 3 M GdnHCl); however, the presence of these species was not reproducible.

An increment in Rs from 36.1 ± 0.8 to 37.8 ± 0.8 Å is observed by DLS measurements (Fig. 5) at the same GdnHCl concentration interval in which dissociation occurs. In agreement with the DLS measurements, the elution volume difference between Peak I and II corresponds to a calculated Rs difference of ~2.5 Å. Since the unfolded state contributes marginally to the total population species at 0.5 M (Fig. 3), the value obtained by DLS at 0.5 M of GdnHCl could correspond to the Rs of the monomeric intermediate.

As expected, the complete unfolding of the intermediate produces a decrement in the elution volume of peak II (as a single peak) and an increment of the Rs from ~38 to 50 ± 2 Å, as measured by SEC and DLS, respectively (Fig. 5). Coincident with our

observations, the calculated Rs of a completely unfolded 33 kDa polypeptide is 53 Å [21].

4. Discussion

4.1. Intersubunit interactions are determinant for the stability of Pfk-2

A three-state unfolding mechanism for Pfk-2, $N_2 \leftrightarrow 2I \leftrightarrow 2U$, was inferred from equilibrium conditions where "I" is a highly populated monomer characterized by residual secondary structure and an expanded volume. The $N_2 \leftrightarrow 2I$ transition involves the concerted loss of enzymatic activity, native environment around Trp-88 residue and about 70% of the native secondary structure, as indicated by the coincidence in the energetic parameters extracted from these structural probes (Table 1).

The structural properties of the monomeric intermediate suggest that it does not fit into the classic molten globule description [22,23]. In agreement with the significant loss of secondary structure, the Rs of the monomeric intermediate (38 Å) is about 13 Å higher than that predicted for a compact monomer of 33 kDa [21]. Indeed, the difference between the observed and calculated Rs of this intermediate goes beyond the reported 15% increment for polypeptides in the molten globule configuration [24]. The unstructured character of this monomeric intermediate is also reflected by the *m*-value of the transition. Theory holds that *m*-values should be approximately proportional to the amount of new surface area, $\Delta A(A_{\text{denatured}} - A_{\text{native}})$, exposed upon unfolding of the native state [25]. Using an empiric approximation [19], *m*-values ranging from 16.4 to 18.4 kcal mol^{-1} M^{-1} can be approximated for complete unfolding of Pfk-2. Since the experimental *m*-values for $N_2 \leftrightarrow 2I$ and $I \leftrightarrow U$ steps were 17 ± 3 kcal mol^{-1} M^{-1} and 1.7 $kcal^{-1}$ mol^{-1} M^{-1}, the monomeric intermediate seems highly hydrated, although the variation of the ANS fluorescence area indicates that a hydrophobic patch remains in its structure. Such kind of properties corresponds to the so called pre-molten globule [26,27].

Homologous members of Pfk-2, like ribokinase, tagatose-6-P kinase, and fructokinase, are homodimers stabilized by an interface created by an orthogonal packing of four-stranded beta-sheets, the β-clasp. This topology reassembles a flatten β-barrel stabilized by a bimolecular hydrophobic core [2]. Since, interfaces that mimic a compact domain suffer concerted unfolding/dissociation reactions [28–30] it seems unlikely that the isolated subunits of Pfk-2 preserve the conformation observed in the context of its dimeric structure. However, the physical characteristics of the monomeric intermediate described above, together with the large *m*-value associated with its formation, suggest that a portion of the protein, larger than the polypeptide chain that conforms the β-clasp interface, could unfold cooperatively with the dissociation of the Pfk-2 subunits. Therefore, the β-clasp interface and an important portion of the conserved α/β/α domain of each subunit could be considered as a single cooperative unit, where the stability of both domains influences each other. To perform a detail study of the effects of neighbouring domains, one has to study the domain in isolation as well as in the two domain protein [31–33]. Isolation of both domains in Pfk-2 and related kinases is troubled since the β-sheet structure is inserted discontinuously into the primary sequence of the α/β/α domain.

4.2. Comparison between the equilibrium unfolding pathway of Pfk-2 with other members of the of the ribokinase superfamily

Few stability studies have been performed with the ribokinase superfamily members and hence little is known about the presence of equilibrium intermediates that could be correlated with the structural determinants of the conserved α/β/α fold. Mammalian pyridoxal kinases have been characterized as active monomers [7] mainly composed by the α/β/α domain since the additional β-sheet is replaced by a small loop that covers the ATP binding site [8,9]. Despite of the marginal percentage of identity between the sequence of pyridoxal kinase and homologues of Pfk-2, the enzymes present a good structural superposition when their conserved α/β/α domains are overlapped [8]. In contrast with the $N_2 \leftrightarrow 2I \leftrightarrow 2U$ equilibrium unfolding mechanism proposed here for Pfk-2, pyridoxal kinase from human [10] and sheep [11] have been reported to unfold through a single transition ($N \leftrightarrow U$), with associated stability values of 2.4 and 1.2 kcal mol^{-1} and *m*-values of 2.4 and 1.2 kcal mol^{-1} M^{-1}, respectively. However, besides the reduced stability, the reported *m*-values obtained for the $N \leftrightarrow U$ transitions are lower than those expected for the full α/β/α domain unfolding of pyridoxal kinase (expected *m*-values are about 8.1 kcal mol^{-1} M^{-1} [19]). This observation was not discussed in the original works, but would indicate the presence of hidden intermediate(s) in the equilibrium unfolding pathway of pyridoxal kinase. Interestingly, the monomeric intermediate of Pfk-2 shows a stability of 2.6 kcal mol^{-1} and a *m*-value of 1.4 kcal mol^{-1} M^{-1} with respect to the unfolded state, but it is not known if this intermediate has a structural counterpart in the equilibrium unfolding pathway of pyridoxal kinase.

Acknowledgements

This work was supported by a grant from the Comisión Nacional de Investigación Científica y Tecnológica, FONDECYT 1050818, Chile. M.B. was supported by Facultad de Ciencias, Universidad de Chile and partially by FONDECYT. We acknowledge the helpful advice of Patricio Rodríguez at the initial stages of this work. We thank Ricardo Cabrera for helpful discussions and for performing the light scattering experiments. The light scattering measurements were performed at the Laboratorio de Cristalografía, Instituto de Física de São Carlos, Universidad de São Paulo, Brazil.

References

[1] Murzin, A.G., Brenner, S.E., Hubbard, T. and Chothia, C. (1995) SCOP: a structural classification of proteins database for the investigation of sequences and structures. J. Mol. Biol. 247, 536–540.
[2] Sigrell, J.A., Cameron, A.D., Jones, T.A. and Mowbray, S.L. (1998) Structure of *Escherichia coli* ribokinase in complex with ribose and dinucleotide determined to 1.8 Å resolution: insights into a new family of kinase structures. Structure 6, 183–193.
[3] Miallau, L., Hunter, W.N., McSweeney, S.M. and Leonard, G.A. (2007) Structures of Staphylococcus aureus D-tagatose-6-phosphate kinase implicate domain motions in specificity and mechanism. J. Biol. Chem. 282, 19948–19957.
[4] Ohshima, N., Inagaki, E., Yasuike, K., Takio, K. and Tahirov, T.H. (2004) Structure of thermus thermophilus 2-keto-3-deoxygluconate kinase: evidence for recognition of an open chain substrate. J. Mol. Biol. 340, 477–489.
[5] Cabrera, R., Ambrosio, A.L., Garratt, R.C., Guixé, V. and Babul, J. (2008) Crystallographic structure of phosphofructokinase-2 from *Escherichia coli* in complex with two ATP molecules. Implications for substrate inhibition. J. Mol. Biol. 383, 588–602.
[6] Zhang, Y., Dougherty, M., Downs, D.M. and Ealick, S.E. (2004) Crystal structure of an aminoimidazole riboside kinase from Salmonella enterica: implications for the evolution of the ribokinase superfamily. Structure 12, 1809–1821.
[7] Kwok, F., Scholz, G. and Churchich, J.E. (1987) Brain pyridoxal kinase dissociation of the dimeric structure and catalytic activity of the monomeric species. Eur. J. Biochem. 168, 577–583.
[8] Li, M.H., Kwok, F., Chang, W.R., Lau, C.K., Zhang, J.P., Lo, S.C., Jiang, T. and Liang, D.C. (2002) Crystal structure of brain pyridoxal kinase, a novel member of the ribokinase superfamily. J. Biol. Chem. 277, 46385–46390.
[9] Safo, M.K., Musayev, F.N., di Salvo, M.L., Hunt, S., Claude, J.B. and Schirch, V. (2006) Crystal structure of pyridoxal kinase from the *Escherichia coli* pdxK gene: implications for the classification of pyridoxal kinases. J. Bacteriol. 188, 4542–4552.
[10] Lee, H.S., Moon, B.J., Choi, S.Y. and Kwon, O.S. (2000) Human pyridoxal kinase: overexpression and properties of the recombinant enzyme. Mol. Cell 10, 452–459.
[11] Pineda, T. and Churchich, J.E. (1993) Reversible unfolding of pyridoxal kinase. J. Biol. Chem. 268, 20218–20222.

[12] Caniuguir, A., Cabrera, R., Baez, M., Vásquez, C.C., Babul, J. and Guixé, V. (2005) Role of Cys-295 on subunit interactions and allosteric regulation of phosphofructokinase-2 from *Escherichia coli*. FEBS Lett. 579, 2313–2318.
[13] Baez, M., Merino, F., Astorga, G. and Babul, J. (2008) Uncoupling the MgATP-induced inhibition and aggregation of *Escherichia coli* phosphofructokinase-2 by C-terminal mutations. FEBS Lett. 582, 1907–1912.
[14] Baez, M., Cabrera, R., Guixé, V. and Babul, J. (2007) Unfolding pathway of the dimeric and tetrameric forms of phosphofructokinase-2 from *Escherichia coli*. Biochemistry 46, 6141–6148.
[15] Cabrera, R., Fischer, H., Trapani, S., Craievich, A.F., Garratt, R.C., Guixé, V. and Babul, J. (2003) Domain motions and quaternary packing of phosphofructokinase-2 from *Escherichia coli* studied by small angle X-ray scattering and homology modeling. J Biol. Chem. 278, 12913–12919.
[16] Pace, C.N. (1986) in: Enzyme Structure, Part L (Hirs, C.H.W. and Timasheff, S.N., Eds.), pp. 266–280, Academic Press Inc.
[17] Babul, J. (1978) Phosphofructokinases from *Escherichia coli*. Purification and characterization of the nonallosteric isozyme. J. Biol. Chem. 253, 4350–4355.
[18] Apiyo, D., Jones, K., Guidry, J. and Wittung-Stafshede, P. (2001) Equilibrium unfolding of dimeric desulfoferrodoxin involves a monomeric intermediate: iron cofactors dissociate after polypeptide unfolding. Biochemistry 40, 4940–4948.
[19] Myers, J.K., Pace, C.N. and Scholtz, J.M. (1995) Denaturant m values and heat capacity changes: relation to changes in accessible surface areas of protein unfolding. Protein Sci. 4, 2138–2148.
[20] Daniel, E. and Weber, G. (1966) Cooperative effects in binding by bovine serum albumin. I. The binding of 1-anilino-8-naphthalenesulfonate. Fluorimetric titrations. Biochemistry 5, 1893–1900.
[21] Uversky, V.N. (1993) Use of fast protein size-exclusion liquid chromatography to study the unfolding of proteins which denature through the molten globule. Biochemistry 32, 13288–13298.
[22] Kuwajima, K. (1989) The molten globule state as a clue for understanding the folding and cooperativity of globular-protein structure. Proteins 6, 87–103.
[23] Arai, M. and Kuwajima, K. (2000) Role of the molten globule state in protein folding. Adv. Protein Chem. 53, 209–282.
[24] Uversky, V.N. (2002) Natively unfolded proteins: a point where biology waits for physics. Protein Sci. 11, 739–756.
[25] Schellman, J.A. (1978) Solvent denaturation. Biopolymers 17, 1305–1322.
[26] Uversky, V.N. and Ptitsyn, O.B. (1996) Further evidence on the equilibrium "pre-molten globule state": four-state guanidinium chloride-induced unfolding of carbonic anhydrase B at low temperature. J. Mol. Biol. 255, 215–228.
[27] Uversky, V.N. and Fink, A.L. (2002) The chicken-egg scenario of protein folding revisited. FEBS Lett. 515, 79–83.
[28] Tsai, C.J. and Nussinov, R. (1997) Hydrophobic folding units at protein-protein interfaces: implications to protein folding and to protein-protein association. Protein Sci. 6, 1426–1437.
[29] Tsai, C.J., Xu, D. and Nussinov, R. (1997) Structural motifs at protein-protein interfaces: protein cores versus two-state and three-state model complexes. Protein Sci. 6, 1793–1805.
[30] Larsen, T.A., Olson, A.J. and Goodsell, D.S. (1998) Morphology of protein–protein interfaces. Structure 6, 421–427.
[31] Batey, S., Randles, L.G., Steward, A. and Clarke, J. (2005) Cooperative folding in a multi-domain protein. J. Mol. Biol. 349, 1045–1059.
[32] Batey, S. and Clarke, J. (2006) Apparent cooperativity in the folding of multidomain proteins depends on the relative rates of folding of the constituent domains. Proc. Natl. Acad. Sci. USA 103, 18113–18118.
[33] Han, J.H., Batey, S., Nickson, A.A., Teichmann, S.A. and Clarke, J. (2007) The folding and evolution of multidomain proteins. Nat. Rev. Mol. Cell Biol. 8, 319–330.